INTERNATIONAL JOURNAL OF HYDROGEN ENERGY 36 (2011) 7602–7611

Available at www.sciencedirect.com

ScienceDirect

journal homepage: www.elsevier.com/locate/he

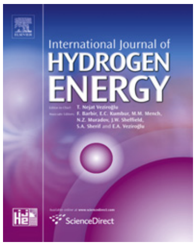

Decomposition of lithium magnesium aluminum hydride

Hilde Grove [a], *Ole Martin Løvvik* [a,1], *Weiming Huang* [b], *Susanne M. Opalka* [c],
Richard H. Heyn [d], *Bjørn C. Hauback* [a,*]

[a] *Institute for Energy Technology, P.O. Box 40, NO-2027 Kjeller, Norway*
[b] *QuesTek Innovations, LLC, 1820 Ridge Avenue, Evanston, IL 60201, USA*
[c] *United Technologies Research Center, 411 Silver Lane, East Hartford, CT 06108, USA*
[d] *SINTEF Materials and Chemistry, P.O. Box 124 Blindern, NO-0314 Oslo, Norway*

ARTICLE INFO

Article history:
Received 10 January 2011
Received in revised form
11 March 2011
Accepted 19 March 2011
Available online 22 April 2011

Keywords:
Hydrogen storage
Metal hydride
Alanates
Complex hydride
Thermodynamic modeling

ABSTRACT

The quaternary aluminum hydride $LiMg(AlH_4)_3$ contains 9.7 wt% hydrogen, of which 7.2 wt% can be released in a two-step decomposition reaction via first formation of $LiMgAlH_6$ and then the binary hydrides MgH_2 and LiH. *In-situ* synchrotron radiation powder X–ray diffraction and thermal desorption spectroscopy measurements were performed to analyze the product distributions formed during the thermal decomposition of $LiMg(AlD_4)_3$. The first decomposition step occurs at about 120 °C and the second at about 160 °C for the as-milled sample, while for a purified sample of $LiMg(AlD_4)_3$, the decomposition temperatures involving release of hydrogen increase to 140 and 190 °C, respectively, suggesting that pure samples of $LiMg(AlD_4)_3$ are kinetically stabilized. Studies of the purified $LiMg(AlD_4)_3$ also showed that the second decomposition step can be divided into two reactions: $3LiMgAlD_6 \rightarrow Li_3AlD_6 + 3MgD_2 + 2Al + 3D_2$ and $Li_3AlD_6 \rightarrow 3LiD + Al + 3/2D_2$. Addition of $TiCl_3$ to $LiMg(AlD_4)_3$ under a variety of ball milling conditions consistently led to decomposition of $LiMg(AlD_4)_3$ during milling. Correspondingly, all attempts to rehydrogenate the (completely or partially) decomposed samples at up to 200 bar hydrogen pressure failed. Decomposition of MgD_2 was observed at relatively low temperatures. This is ascribed to thermodynamic destabilization due to the formation of different Al_xMg_y phases, and to kinetic destabilization by addition of $TiCl_3$. A thermodynamic assessment was established for the calculation of phase stability and decomposition reaction relationships within the Li–Mg–Al–H system. The calculations confirmed the metastability of the $LiMg(AlH_4)_3$ phase and the irreversibility of the Li–Mg alanate phase decomposition reactions. The Li–Mg alanate decomposition pathways followed experimentally could be explained by the endothermicity of the calculated decomposition enthalpies, in that an impure or catalyzed $LiMgAlH_6$ intermediate phase could more directly access an endothermic decomposition reaction at lower temperatures, while a kinetically-hindered, purified $LiMgAlH_6$ would require higher temperatures to initiate the two-step decomposition through an exothermic reaction.

1. Introduction

Hydrogen storage in solid compounds is considered to be the only storage method that will meet the long-term goals for hydrogen storage for mobile applications [1]. One of the most attractive groups of materials is that of the lightweight, high gravimetric capacity aluminum-based hydrides (alanates), some of which have a theoretical capacity of up to 11 wt%

---

[*] *Corresponding author*. Tel.: +47 63 80 60 78; fax: +47 63 81 09 20.
E-mail address: bjorn.hauback@ife.no (B.C. Hauback).
[1] Present address: SINTEF Materials and Chemistry, P.O. Box 124 Blindern, NO-0314 Oslo, Norway.

doi:10.1016/j.ijhydene.2011.03.110

H_2 [2]. The reversibility and improved kinetics found in Ti-enhanced sodium alanate $NaAlH_4$ by Bogdanović and Schwickardi initiated a significant effort on alanates [3]. The theoretical gravimetric density of $NaAlH_4$ is 5.6 wt% H_2, which is considered too low for transportation purposes. A potential alternative is lithium magnesium tetra-alanate $LiMg(AlH_4)_3$, which contains 9.7 wt% H_2, whereof 7.2 wt% is released upon decomposition to the binary hydrides. $LiMg(AlH_4)_3$ can be produced mechanochemically by mixing $LiAlH_4$ and $MgCl_2$ [4–6], followed by removal of co-produced LiCl by extraction with organic solvents (Eq. (1)).

$$3\,LiAlH_4 + MgCl_2 \rightarrow LiMg(AlH_4)_3 + 2\,LiCl \tag{1}$$

A two-step pathway was found for the decomposition of $LiMg(AlH_4)_3$. In the first decomposition reaction (Eq. (2)), 4.8 wt% H_2 is released, and in the second decomposition reaction (Eq. (3)) 2.4 wt% H_2 is released from the intermediate lithium magnesium hexa-alanate $LiMgAlH_6$ [5,6].

$$LiMg(AlH_4)_3 \overset{120^{\circ}C}{\rightarrow} LiMgAlH_6 + 2\,Al + 3\,H_2 \tag{2}$$

$$LiMgAlH_6 \overset{160^{\circ}C}{\rightarrow} LiH + MgH_2 + Al + 3/2H_2 \tag{3}$$

An additional 2 wt% H_2 can be released from the decomposition of MgH_2 to Mg and H_2 at 250 °C and above. The crystal structures of the corresponding deuterides, $LiMg(AlD_4)_3$ and $LiMgAlD_6$, have been determined recently [7,8]. The $LiMg(AlD_4)_3$ structure consists of isolated AlD_4 tetrahedra connected through octahedral Mg- and Li-ions, while the $LiMgAlD_6$ structure consists of isolated AlD_6 octahedra connected through octahedral Mg- and Li-ions. Recently the effect of graphitic nanofibres for improving the desorption kinetics of $LiMg(AlH_4)_3$ has been studied [9].

The scope of this work was to investigate the thermodynamic stability of the Li–Mg alanates and their decomposition reactions, by application of both experimental and theoretical methods. Temperature programmed desorption (TPD) was performed to characterize the Li–Mg alanate dehydrogenation profiles, and *in-situ* synchrotron radiation X–ray diffraction studies (SR–PXD) were performed for additional phase analyses. The potential enhancement of the Li–Mg alanate kinetics was investigated by the addition of $TiCl_3$ via mechanochemical milling at room temperature, at liquid nitrogen temperature, and at high H_2 pressure. Rehydrogenation was attempted using H_2 pressures up to 200 bar. Thermodynamic modeling was used to interpret the experimentally observed phase behavior, and a thermodynamic assessment of the Li–Mg–Al–H quaternary order system was made using published experimental data. This assessment was evaluated by comparison with thermodynamic properties predicted by first principles atomic modeling. The experimental assessment parameters were used to model the energetics and equilibrium H_2 pressures of the possible decomposition reactions within the Li–Mg–Al–H system.

2. Methodology

2.1. Synthesis and Instruments

All chemicals were purchased from commercial sources: $LiAlD_4$ (>98 atom% D and chemical assay >95%; Sigma–Aldrich), $MgCl_2$ (99.9% Sigma–Aldrich), $TiCl_3$ (>99.99, Sigma–Aldrich); and used as received. The deuterated lithium alanate, $LiAlD_4$, was used since high purity $LiAlH_4$ is not commercially available. Toluene was dried over Na/anthracene and distilled under argon, and Et_2O was dried over Na/benzophenone and distilled under argon.

$LiMg(AlD_4)_3$ was synthesized by milling $LiAlD_4$ and $MgCl_2$ (ratio 3:1) in a Fritsch P6 planetary rotary ball mill at 300 rpm for 3 h, using a ball:powder ratio of 200:1, and was recrystallized and purified as described earlier [7]. All handling of the samples was performed under argon, using a glove box with less than 1 ppm O_2 and H_2O. Four different milling procedures were used for the addition of $TiCl_3$: high intensity, low intensity, cryogenic, and high-pressure milling. The former two were performed using the Fritsch P6 planetary ball mill, with a 250 ml grinding bowl and a GTM sensor lid measuring the pressure during milling (certified up to 5 bar). The typical sample mass was 2 g. High intensity (HI) ball milling was performed at 300 rpm for several hours, with excess pressure released during milling. Low intensity (LI) ball milling was done at 150 rpm with a repeated series of 15 min milling interrupted by 5 min pauses. Cryogenic milling (cryomilling, CM) was performed in an SPEX 6750 freezer mill where liquid nitrogen is used to cool a steel container with the sample and a stainless steel cylindrical impactor. The impact frequency was 30 Hz, and the impactor mass was 32 g. CM was performed using 6 min milling time with subsequent cooling time of 3 min to prevent heating of the system. This was repeated 9 times, giving an effective milling time of 54 min. High-pressure (HP) ball milling was performed using an in-house built milling vial, at 70–75 bar H_2 pressure. The speed was 300 rpm and the milling time was 15 min with 5 min pauses. Variable total milling times were used, and the typical ball:powder ratio was 24:1. Details of the syntheses of the different samples studied are available in the Supporting Information.

TPD was performed with an in-house built setup. Different quantities (0.1–0.5 g) and heating rates (0.25–5 K/min) were used depending on the sample. The experiments were generally performed under dynamic vacuum; in some experiments samples were desorbed into a constant volume. Pressure–Composition–Temperature (PCT) experiments were performed using an in-house built Sieverts apparatus equipped with a pressure sensor from Presens [10] and is operable up to 200 bar and 600 °C.

Initial powder X–ray diffractometer (PXD) data for inspecting phase compositions were obtained with an INEL XRG 3000 with Cu $K\alpha_1$ radiation ($\lambda = 1.540598$ Å), Ge crystal monochromator, and Inel CPS 120, a curved position sensitive detector. Time resolved *in-situ* SR–PXD data were collected at the Swiss-Norwegian beamline (SNBL, station BM1A) at the European Synchrotron Radiation Facility (ESRF) in Grenoble, France. Two-dimensional data with an exposure time of 30 s were collected with an imaging plate (MAR345) detector. Wavelengths between 0.7 and 0.8 Å were used. The samples were packed in boron-silica-glass capillaries and connected to a vacuum pump using Swagelok fittings. The samples were heated using a hot air blower with heating rates in the range 0.25–4 K/min from room temperature (RT) up to 400 °C, and data were collected every second minute. The temperatures were calibrated using an Ag-standard and by determining the